100 KIEE International Transactions on PE, Vol. 3-A No. 2, pp. 100~108, 2003

Design and Test Results of 6-kA HTS-Copper Current Leads with HTS Section Operating in the Current-Sharing Mode

Haigun Lee*, Ho Min Kim*, Yukikazu Iwasa*, Keeman Kim**
Paul Arakawa*** and Greg Laughon*****

Abstract - This paper presents the design and performance results of a pair of 6-kA high-temperature superconducting (HTS)-copper current leads, in which, over a short length at the warm end (e.g., 77K) of each HTS section, comprised of paralleled Bi-2223/Ag-Au tapes, is operated in the *current-sharing* mode. Because of their reliance on vapor cooling, the leads are applicable only to liquid helium cooled superconducting magnets such as those used in high-energy physics accelerators and fusion machines. The experimental measurements have demonstrated that key performance data of the new 6-kA HTS-Copper leads agree reasonably well with those expected from design.

Keywords: high-temperature superconducting (HTS) current lead; Bi-2223/Ag-Au tapes

1. Introduction

Current leads presently available that incorporate high-temperature superconducting (HTS) sections are, though effective in reducing liquid helium boil off rates, bulky and expensive in comparison with copper-based gas-cooled leads. What is needed is a new HTS section that, while keeping efficient thermal performance, results in a compact and affordable lead. Our recent analysis [1] and design/performance [2] have demonstrated that the new HTS sections are compact and thermally efficient. The new HTS/Copper Leads are applicable only to liquid helium cooled superconducting magnets such as those used in large high-energy particle accelerators and magnetically confined fusion devices. The new integrated HTS/Copper leads that we believe can be made affordable should significantly improve the cryogenic efficiency of these systems. Compactness of the leads should also facilitate retrofitting existing current leads with these new leads.

This paper describes the design procedure, parameters, and performance results of the new 6-kA HTS-Copper leads built by AMI and tested at MIT. The leads were designed by MIT based on a new concept described elsewhere [1,2].

* MIT Francis Bitter Magnet Laboratory (FBML), Cambridge, MA 02139, U.S.A. (hlee@jokaku.mit.edu)
** Nuclear Fusion R&D Center, Korea Basic Science Institute (KBSI), Korea (kkeeman@kbsi.re.kr)
*** American Magnetics, Inc.(AMI), Oak Ridge, TN 37831, U.S.A.
Received February 4, 2003 ; Accepted March 26, 2003

2. Design procedure for HTS section

2.1 Design Procedure for the HTS Section - Iteration 1

Given below is a step-by-step procedure for design of the HTS section of a new pair of 6-kA HTS-Copper leads. In Iteration 1, a protection requirement is not included.

Step 1: Parameters of Bi-2223/Ag-Au Tape Key parameters of Bi-2223/Ag-Au tape are: 1) overall dimensions: width; thickness; and Bi-2223 filling (volume, in %); 2) critical currents in self field: $i_c(T_l)$ and $i_c(T_0)$, both at a normal field, $B_\perp$ = 0.2 T corresponding to this pair of 6-kA leads; 3) Ag-Au alloy: Au content; cross sectional area, a_m; T-averaged thermal conductivity, k_m, in the range T_0-T_l; and T-averaged electrical resistivity, ρ_m. Table 1 presents these parameters.

Step 2: Bi-2223/Ag-Au Quantity The number of HTS tape, N_{tp}, is determined by $I_c(T_l) = N_{tp} i_c(T_l)$, where $I_c(T_l)$ is the critical current at the warm end and i_c(@77.3 K and $B_\perp$ = 0.2 T) = 80 A. Although values of N_{tp} as small as 38 (50%) may be selected for our HTS section, N_{tp} = 60 (80% of that required for a *Fully-Superconducting* (*FullSuper*) version requiring N_{tp} = 75) was selected.

Step 3: Current-Sharing Temperature Once $I_c(T_l)$ is selected, the current-sharing temperature, T_{cs}, may be determined. For this, it is assumed that $I_c(T) \equiv N_{tp} i_c(T)$ is a linear function of T, decreasing linearly from $I_c(T_0) = N_{tp} i_c(T_0)$ to $I_c(T_l)$. From this linear function, we may determine T_{cs}, at which point $I_t = I_c(T_{cs})$.

Table 1 Parameters of AMSC Bi-2223/Ag-Au Tape

Parameters		*Value*
Overall width	[mm]	4.2
Overall thickness	[mm]	0.228
Bi-2223 filling (volume)	[%]	42
Au content	[wt%]	5.3
Ag-Au cross section, a_m	[mm^2]	0.555
{a_{tp} (tape cross section)}	[mm^2]	0.958
$i_c(T_l)$ (@77.3 K @B$_\perp$ = 0.2 T)	[A]	80*
$i_c(T_0)$ (@4.2 K @B$_\perp$ = 0.2 T)	[A]	450†
k_m (4.2~77 K)	[W/cm K]	0.327
ρ_m (4.2~77 K)	[μΩcm]	1.0

* 1-μV/*cm* criterion.

† Note that at 4.2 K the effect of B$_\perp$ = 0.2 T is negligible

Step 4: Design of FullSuper Version First, design a *FullSuper* counterpart for a given combination of Q_{in} and l, which are related by:[1]

$$Q_{in} = \frac{k_m A_m h_L}{C_P l} \ln\left[\frac{C_P(T_l - T_0)}{h_L} + 1\right] \tag{1}$$

In Eq. 1 A_m is the total cross sectional area of the Ag-Au alloy, given by $A_m = N_{tp} a_m$.

With h_L=20.4 J/g (liquid helium at 4.2 K); C_p = 5.280 J/g·K (helium vapor, 4.2~80 K); T_0 = 4.2 K; and T_l = 77.3 K, a value of Q_{in} may be computed from Eq. 1 for a given choice of l. For l = 19.5 cm: $Q_{in} \geq 0.065$ W for 6-kA. Because for standard AMI vapor-cooled copper leads rated 6-kA, $Q_{in} \approx 7.2$ W/lead, reduction in Q_{in} achievable with HTS-Copper leads can exceed a factor of 100.

Step 5: Protection Criterion Before proceeding further, it is appropriate at this point to introduce a protection criterion in the design. Here we review a fault-mode scenario for protection of a vapor-cooled current lead: flow stoppage.

We may analyze this condition by assuming the adiabatic condition in which Joule heating is converted to raising the lead temperature: [3]

$$\rho_m(T) J_m^2(t) = C_{tp}(T) \frac{dT_m(t)}{dt} \tag{2}$$

where $\rho_m(T)$ and $J_m(t)$ are, respectively, the resistivity and current density of the matrix; $C_{tp}(T)$ is the heat capacity of the tape (Bi-2223 and Ag-Au); and $T_m(t)$ is the matrix temperature. Based on the assumption that $C_{bi2223}(T) \approx C_{ag\text{-}au}(T)$, with the 58 %/42 % = 1.38 to take into account the volumetric ratio of this tape, we may assume $C_{tp}(T) \approx 1.38 C_m(T)$ and integrate Eq. 2 in time and temperature as given below:

$$\int J_m^2(t)dt \cong 1.38 \int_{T_i}^{T_f} \frac{C_m(T)}{\rho_m(T)} dT \cong 1.38 \frac{\Delta H_m(T_i, T_f)}{\rho_m} \tag{3}$$

where $\Delta H_m(T_i,T_f)$ is the total change in enthalpy of the matrix between T_i and T_f. The second approximation of Eq. 3 is valid for alloys whose resistivity is nearly constant over this temperature span. The left-hand side of Eq. 3 may be divided into two time segments, first between t = 0 (start of flow stoppage) and $t = \tau_{del}$ (delay in discharge action), and second between $t = \tau_{del}$ and $t = \tau_{del} + \tau_{dis}$, where τ_{dis} is the exponential discharge time constant. From Eq. 3, we may derive a protection criterion for an HTS section:

$$J_{mo}^2 \tau_{del} + \frac{1}{2} J_{mo}^2 \tau_{dis} \leq 1.38 \frac{\Delta H_m(T_i, T_f)}{\rho_m} \tag{4}$$

where $J_{mo} \equiv I_t/A_m$ is the matrix current density in at t = 0.

We apply Eq. 4 to the *FullSuper* HTS section, which for $A_m = 60 a_m = 0.333$ cm^2 has a value of J_{mo} = 18.02 kA/cm^2. The left-hand side of Eq. 4, for τ_{del} = 5 s and τ_{dis} = 25.6 s, for example, is thus 57.8×10^8 A^2 s/cm^4.

With T_i = 77 K, T_f = 200 K, and $\rho_m = 1\times10^{-6}$ Ωcm, the right-hand side of Eq. 4 is 3.6×10^8 A^2·s/cm^4 for the enthalpy and density of silver. Clearly, the protection criterion of Eq. 4 is *not* met even by the *FullSuper* version rated at 6-kA.

2.2 Design Procedure – Iteration 2

Step 0: Parameters of Bi-2223/Ag-Au Tape The parameters of Bi-2223/Ag-Au tape are identical to those in the Iteration 1 design given in Table 1.

Step 1: Protection Requirement—Left-Hand Side of Eq. 4 Because even the total matrix cross sectional area of 0.333 cm^2 (6-kA) for the *FullSuper* HTS section is utterly inadequate to satisfy the condition of Eq. 4, it is necessary to introduce in each HTS section an additional normal metal (NM) element, thereby reducing J_{mo}. The total NM cross section area, A_{nm}, may be determined from Eq. 4. By neglecting A_m, we may express the left-hand side of Eq. 4 by the following expression:

$$\left(\frac{I_t}{A_{nm}}\right)^2 \tau_{del} + \frac{1}{2}\left(\frac{I_t}{A_{nm}}\right)^2 \tau_{dis} = \left(\frac{I_t}{A_{nm}}\right)^2 \left(\tau_{del} + \frac{1}{2}\tau_{dis}\right) \tag{5}$$

Right-Hand Side of Eq. 4 This normal metal must have the following properties.

1. Low T-averaged electrical resistivity, ρ_{nm}. Note that a

low value of ρ_{nm} will enhance the right-hand side of Eq. 4.

2. Low T-averaged thermal conductivity, k_{nm}. Note that k_{nm} will appear in a new expression for Q_{in} similar to Eq. 1.

3. Common material and readily available in tape form.

4. Easily solderable to Bi-2223/Ag-Au tape.

A potential candidate for this metal is brass, key properties of which are as follows.

1. $\rho_{nm} = 2.84\times10^{-6}$ Ωcm in the range 77-200 K; 2.25×10^{-6} Ωcm (4.2~77 K) [4].

2. $k_{nm} = 0.35$ W/K·cm in the range 4.2-77 K.

Approximating brass (Cu-Zn) as copper, we obtain for T_i = 77 K and T_f = 200 K:

$$\left(\frac{I_t}{A_{nm}}\right)^2\left(\tau_{del}+\frac{1}{2}\tau_{dis}\right)\le 1.14\times10^8[A^2s/cm^4] \tag{6}$$

With τ_{del} = 5 s and τ_{dis} = 25.6 s: A_{nm} = 2.37 cm^2 for 6-kA lead. This value is applicable to each of the new 6-kA HTS-Copper leads built by AMI and tested at MIT.

Step 2: Bi-2223/Ag-Au Quantity The numbers of tapes in a *FullSuper* version and the new 6-kA leads are the same as those of the Iteration 1 design.

Configuration Because this extra NM element required by protection should also be vapor-cooled and because Bi-2223/Ag-Au is in the form of paralleled tapes, the extra NM element too should be in the form of paralleled tapes, each NM tape soldered preferably to each superconductor (SC) tape to enhance heat exchange performance.

Dimensions of NM Tape A thickness of 0.445 mm (17.5 mil) and a width of 4.45 mm is chosen for each NM tape.

Step 3: Current-Sharing Temperature This step is identical to that in Iteration 1. For the 6-kA HTS-Copper leads T_{cs} is 72.1 K. For *FullSuper* versions, T_{cs} is always at 77.3 K, because, by definition, no current-sharing regions exist in the *FullSuper* versions.

Step 4: FullSuper Version With this normal metal included, Eq. 1 is modified to:

$$Q_{in} = \frac{(k_m A_m + k_{nm} A_{nm})h_L}{C_P l}\ln\left[\frac{C_P(T_l - T_0)}{h_L}+1\right] \tag{7}$$

Equation 7 gives: Q_{in} = 0.56 W for 6-kA, nearly 10 times greater than that computed in the Iteration 1 design. The new values of Q_{in} are still less than 1/10 those of corresponding AMI standard 6-kA vapor-cooled copper leads.

Step 5: Current-Sharing Regime The current sharing regime spans from $z = l_{cs}$ to $z = l$ (T_0 is at z = 0 and T_l at z = l). Normalized to l, z becomes ξ, l to 1, and l_{cs} to ξ_{cs}. ξ_{cs} may be determined by satisfying the following equation, in which the only unknown is ξ_{cs} for a given set of α_{cs} and β_{cs} defined below [1]:

$$e^{\frac{\alpha_{cs}}{2\xi_{cs}}}\sin\left[\frac{\beta_{cs}(1-\xi_{cs})}{\xi_{cs}}\right] = \frac{\beta_{cs}\left(e^{\alpha_{cs}}-1\right)(T_l - T_{cs})}{\alpha_{cs}e^{\frac{\alpha_{cs}}{2}}(T_{cs}-T_0)} \tag{8}$$

where [1]

$$\alpha_{cs} \equiv \frac{m_{he}C_P l_{cs}}{(k_m A_m + k_{nm}A_{nm})} = \ln\left[\frac{C_P(T_{cs}-T_0)}{h_L}+1\right] \tag{9}$$

Because of the presence of the normal metal element, β_{cs} is modified [1]:

$$\beta_{cs} = \sqrt{\frac{\rho_n\rho_{nm}I_t(I_t - I_{cl})}{(k_n A_n + k_{nm}A_{nm})(\rho_n A_n + \rho_{nm}A_{nm})(T_l - T_{cs})} - \frac{1}{4}\left(\frac{m_{he}C_P}{k_n A_n + k_{nm}A_{nm}}\right)^2} \tag{10}$$

Step 6: HTS Section Length The total HTS section length, l, may be given by $l = l_{cs}/\xi_{cs}$, where ξ_{cs} is determined from Eq. 8 and l_{cs} is determined from the first expression of Eq. 9 for a given value of m_{he}, which is equal to Q_{in}/h_L.

Step 7: Heat Exchange Requirements Stable operation of a vapor-cooled lead, HTS section or copper section, is possible only when the total required cooling power is properly heat-exchanged with the active element of the lead. One parameter that can gauge heat exchange performance is an effective cooling flux, q_{ef}, in the lead. q_{ef} may be given by the total cooling power divided by the total surface area of the element exposed to cooling. Based on performance of standard AMI vapor-cooled copper leads, q_{ef} values 100 mW/cm^2 or less are considered adequate.

For each HTS section, q_{ef} may be given by:

$$q_{ef} = \frac{m_{he}C_P(T_l - T_0)}{N_{tp}lw_{nm}} \tag{11}$$

where w_{nm} is the NM tape width. In Eq. 11, it is assumed, to enhance heat exchange (or to reduce q_{ef}), that each superconductor (SC) tape is soldered to an NM tape; each NM tape may thus be regarded as a fin to the SC tape. Note that in Eq. 11, to be conservative, $N_{tp}lw_{nm}$, which represents one *half* of the total surface of NM tapes theoretically exposed to the cooling vapor, is used to compute q_{ef}. The values of q_{ef} computed, 20.2 mW/cm^2, are well below ~100 mW/cm^2. If q_{ef} values turn out to be greater than ~100 mW/cm^2, then it may require another iteration process.

3. Parameters of 6-kA HTS/Copper leads

Table 2 presents key parameters of 6-kA HTS sections

based on the Iteration 2 design: *FullSuper* in Column 2 and the new HTS section in Column 3. The table shows that the amount of HTS tape required by the new lead, for the same Q_{in} as that of the *FullSuper* versions, is 80% of that required by the *FullSuper* version related at the same current.

As inferred from the table, tape length becomes shorter as N_{tp} is reduced – more saving of SC is possible. Because q_{ef} is essentially determined by A_{nm}, which in turn is dictated by protection requirements, it is possible to reduce N_{tp} even further than 50 % without violating either protection or heat-exchange requirements.

Table 3 presents key parameters of the copper section of the new 6-kA HTS-Copper lead. Note that this lead has Q_{in} ≈ 7.2 W at the 77-K cold end, which, when divided by h_L =20.4 J/g (latent heat of vaporization of helium), gives m_{he} ≈ 0.35 g/s. Because LN2's latent heat of vaporization is 199.3 J/g, its contribution is included in the cooling power and we have: m_{fl} ≈ 0.96 g/s.

Table 2 6-kA HTS Sections-Iteration 2

Parameter		*FullSuper*	*New HTS*
# tapes, SC & NM (N_{tp})		75	60
$I_c(T_l)$ (@77.3K)	[kA]	6	4.8
Ag-Au area, A_m	[cm^2]	0.417	0.333
Q_{in}	[W]	0.56	
NM tape area, A_{nm}	[cm^2]	2.37	
T_{cs}	[K]	77.3	72.1
L	[cm]	19.5	19.5
l-l_{cs}	[mm]	0	4.6
ρ_m; ρ_{nm}	[μΩcm]	1.0; 2.25	
k_m; k_{nm}	[W/Kcm]	0.327; 0.35	
NM tape width†	[mm]	4.45	4.45
Cooling flux	[mW/cm^2]	20.2	20.2
Required HTS tape‡		1	0.80

† For tape thickness of 0.445mm.

‡ Normalized to *FullSuper*.

Table 3 6-kA Copper Section

Parameters		*Value*
Operating range	[K]	77~293
Active area, A_{cu}	[cm^2]	1.19
Active length, l_{cu}	[cm]	38
Cooling area	[cm^2]	12,650
Cooling Mass Flow Rate		
LN2, m_{fl}	[g/s]	0.96
$m_{fl}C_{fl}\theta_l$	[W]	216
Effective Heat Flux		
q_{ef}	[mW/cm^2]	17

4. Experimental Setup & Procedure

4.1 Cryogenics

Fig. 1 shows a schematic diagram for both He and N2 flow lines in the experimental setup. For the sake of clarity, only the flow lines for one lead are shown.

Helium At the start of the experiment, with the test cryostat's outer LN2 reservoir filled, LHe was transferred into the cryostat. The LHe was filled up to a level just below the HTS/bus-bar junction. Because of a relatively large diameter of the LHe section of the cryostat, each 1 cm of LHe level corresponds to ~0.8 liter of liquid. It was possible to remove the transfer line from the cryostat after filling was completed.

As shown in Fig. 1, effluent helium vapor from the bath was forced through the paralleled HTS sections, leaving from the top ends of the HTS sections at ~77 K. The 77-K vapor exiting from each HTS section was guided through a stainless pipe, leaving relatively cold from the top end of the cryostat. The cold vapor was heat-exchanged with the ambient and the two separate flows from each HTS sections were joined before introduced to a vapor volume flow meter to then exhaust from system.

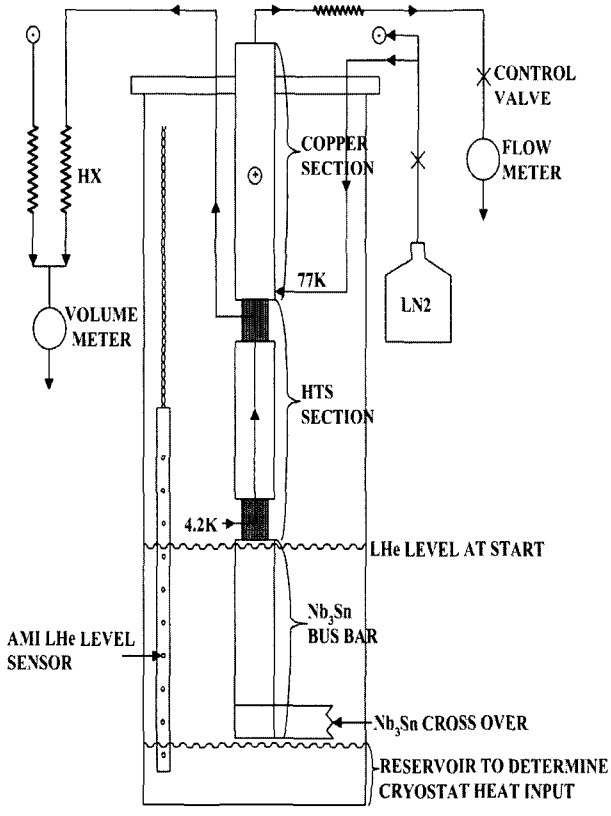

Fig. 1 Schematic diagram for both He and N2 flow lines in the experimental setup. For the sake of clarity, only the flow lines for one lead are shown.

The total boil-off rate of LHe for computation of heat input to the LHe bath was measured from change in fluid level, indicated by an AMI level installed in the system. The vapor volume flow meter reading, because of its strong dependence on vapor temperature, is not suitable for accurate determination of heat input.

Nitrogen LN2 was introduced the bottom end of each copper section. The exhaust vapor from the top end of each section was heat-exchanged with the ambient before it was passed through a flow rate meter. The rate of LN2 flow in each copper section was adjusted to make a vapor flow rate to be near 100 ft^3/h, which corresponds to a designed LN2 flow rate of 4.3 liter/h.

4.2 Electrical

Fig. 2 shows a schematic diagram for the system's electrical requirements for one lead (+). As indicated in the figure, two current ranges were used for measurement: 1) 0~1000 A and 2) 0~6000 A.

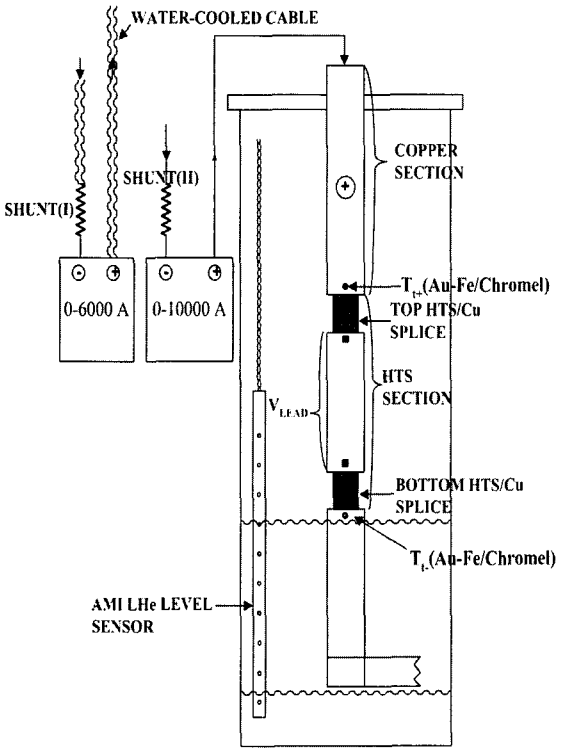

Fig. 2 Schematic diagram for the system's electrical requirements for one lead (+). As indicated in the figure, two current ranges were used for measurement: 1) 0~1000 A and 2) 0~6000 A.

The lead current was measured as the output voltage of either one of the power supplies. Voltages measured for each HTS section include: 1) $V_{lead}(I)$; 2) thermocouple (Au-Fe/chromel) outputs near the top and bottom HTS/Cu splices; and 3) output voltage from the AMI level sensor.

4.3 New 6-kA HTS-Copper Leads

Fig. 3 shows a photograph of a pair of 6-kA HTS-Copper leads, each comprised of: 1) copper lead (77K–RT); 2) HTS section (4.2–77K); 3) Cu/Nb_3Sn composite bus bar (~4.2 K): 4) coolant (liquid N2) inlet pipes; and 5) He-vapor exhaust pipes. Note that the helium and nitrogen are not mixed. Fig. 4 shows a photograph of experimental setup for measurement up to a transport current of 6000 A.

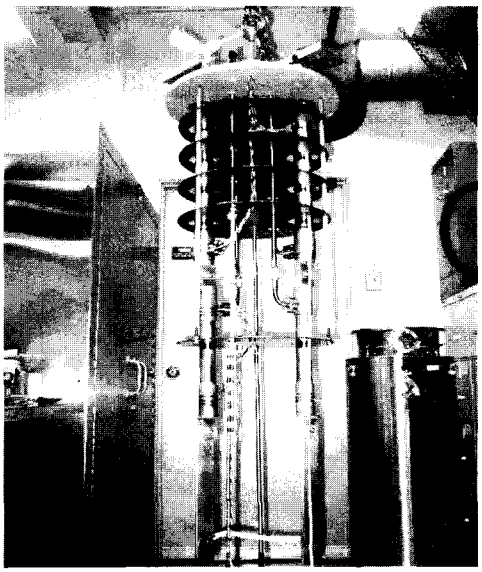

Fig. 3 Photograph of a pair of 6-kA HTS-Copper leads, each comprised of: 1) copper lead (77K–RT); 2) HTS section (4.2–77K); 3) Cu/Nb_3Sn composite bus bar (~4.2 K): 4) coolant (liquid N2) inlet pipes; and 5) He-vapor exhaust pipes.

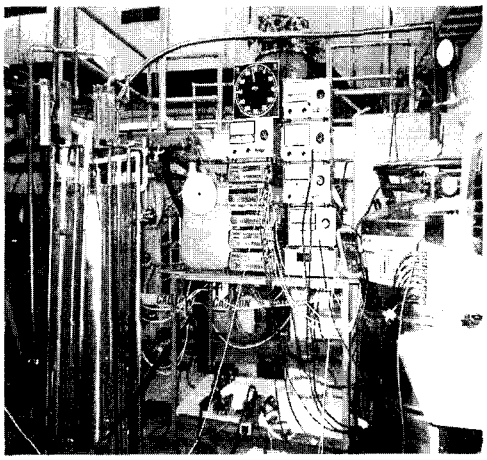

Fig. 4 Photograph of experimental setup for testing up to a transport current of 6000 A.

Each HTS section was extended at its cold end with a 30.6-cm long Nb_3Sn/copper composite bus bar. The bus bar, immersed in liquid helium over most of its length during operation, was shunted at the other end with Nb_3Sn tape to its companion bus bar.

5. Experimental Results

5.1 Experimental Determination of $Q_{in}(I)$

The total heat input to the LHe in the test cryostat, $Q_{tt}(I)$, comprise of two components: 1) $2Q_{in}(I)$, the total heat due to the two 6-kA leads (a factor of 2 for the two HTS sections); and 2) extraneous sources of heat, expressed as Q_{ex}, which unlike $Q_{in}(I)$, is assumed independent of I. In the experiment, $m_{he}(t)$ was determined from the time rate of change of the liquid helium level, dz_{he}/dt, measured with an AMI level sensor. Thus:

$$m_{he}(I) = -A_{lq}\rho_{lq}\frac{dz_{he}}{dt} = \frac{Q_{tt}}{h_L} = \frac{2Q_{in}(I)+Q_{ex}}{h_L} \qquad (12)$$

The negative sign is required because the dz_{he}/dt is negative. Where A_{lq} and ρ_{lq} are, respectively, cross sectional area of the liquid helium in the cryostat and the liquid helium density at 4.2 K. It is quite accurate to assume $A_{lq}=A_{cy}$ where A_{cy} is the test cryostat cross sectional area. Solving Eq. 12 for $Q_{tt}(I)$, we obtain:

$$Q_{tt}(I) = -h_L A_{lq}\rho_{lq}\frac{dz_{he}}{dt} \qquad (13)$$

5.2 Boil-Off and Other Dissipation Data

Fig. 5 shows raw data obtained with the new 6-kA HTS-Copper leads tested up to a transport current of 6000 A. Each set of data is discussed briefly.

Closed Circles The closed circles correspond to Q_{tt}, which comprises $2Q_{in}(I)$ and Q_{ex}.

Shadow Zone The shadow zone represents Q_{ex} of the test cryostat. This was determined with I = 0 and *after* the LHe level in the test cryostat had dropped below the Nb_3Sn shunt at the bottom of the HTS extension. With no part of the 6-kA HTS-Copper leads below the LHe level, Q_{ex} clearly does not contain conductive heat contribution of the leads.

V_{lead}×I Curves Each of the two *VI* curves, LEAD(+) and LEAD(−), represents dissipation generated at the HTS /Copper splices, one at the top and the other at the bottom end of each HTS section. Note that even the bottom splices were always above the LHe during measurement. At 6000 A, the two splices of each HTS section generates ≈2.75 W or a total of 5.5 W. Because the *measured* Q_{tt} at 6000 A was 2.9 W, clearly most of 5.5 W did not enter into the LHe bath. However, because each bottom end splice is thermally well connected to its respective cold-end extension, a fraction of ~1.4 W (=2.75/2 W) might have easily entered into the bath. We believe this is responsible for a slight departure of the measured Q_{tt} from 2.5 W for I >2000 A.

Fig. 6 shows $V(I)$ plot over the range 0~1000 A across one HTS section that includes both top and bottom HTS/Copper splices. Because over this current range, the HTS is completely superconducting, a combined total resistance, 60 nΩ, for this HTS section, may be considered due entirely to the two splices.

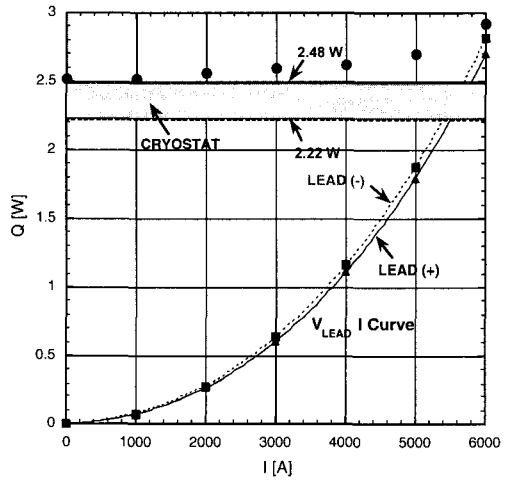

Fig. 5 Raw data. The closed circles correspond to $Q_{tt}(I)$. The shadow zone represents the measured range of Q_{ex}. Each V_{lead}×I curve represents dissipation due chiefly to the splice resistances at the top and bottom HTS/Copper couplings in each HTS section.

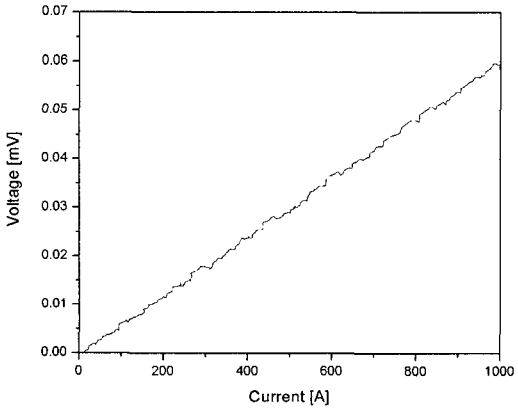

Fig. 6 $V(I)$ plot in the 0~1000 A range across one HTS section containing both top and bottom HTS/Copper splices. In this range HTS section is completely superconducting and the voltage is due entirely to the two splices, which has a combined effective resistance of 60 nΩ.

Fig. 7 shows $V(I)$ plots in the range 0~6000 A for the two HTS sections. For each plot the dashed linear line corresponds to V due to the two HTS/Copper splices. The departure from this dashed line demonstrates appearance of the current-sharing region in the HTS section. Although each of 60 AMSC Bi-2223/Ag-Au tapes has an i_c specification of 100 A (77 K; *self field*), a combination of variation in i_c received from AMSC and degradation in i_c incurred during the brass strip soldering process resulted in a large variation in i_c (77 K; *self field*), as low as 60 A and some as high as 120 A. i_c is further depressed by another 20 % when the effect of $B_\perp$ = 0.2 T is included. Therefore, it is not surprising to observe the current-sharing region occurring at a total current of ~2200 A for the + section and ~2500 A for the – section.

5.3 Temperature Data

The measured temperatures of both bottom and top end of each HTS section, within an experimental uncertainly of ~0.5 K, were independent of current and remained, respectively, at 4.2 K and 77 K.

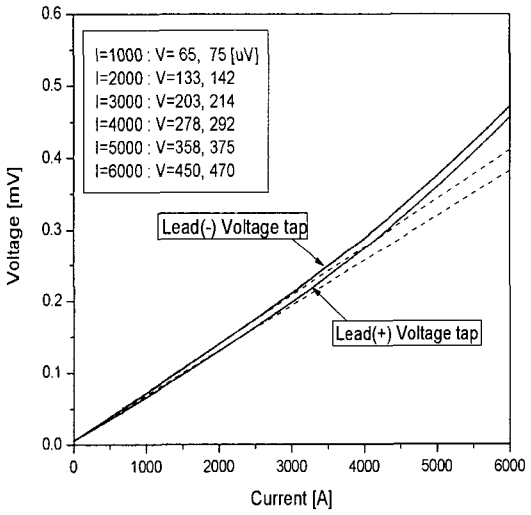

Fig. 7 $V(I)$ plots in the 0~6000 A range across both HTS sections, each containing both top and bottom HTS/Copper splices. The dashed line for each plot corresponds purely resistive contribution from the splices. The departure from each dashed line indicates the current-sharing region in each HTS section.

5.4 LN2 Supply Rate

Each copper section was supplied with LN2 at a flow rate roughly equal to 0.96 g/s (4.3 liquid liter/h), which is equivalent to a room-temperature vapor flow rate of ~100 ft^3/h. Indeed the LN2 supply rate was set to make the outlet vapor flow rate to be ~100 ft^3/h during the measurement.

6. Discussion of Results

We may derive the following results the data.

- From Fig. 5, we may extract $2Q_{in} \leq 0.28$ W given by $Q_{tt}(0) = 2.5$ W subtracted by the minimum extraneous heat input, $Q_{ex} = 2.22$ W or $Q_{in} \leq 0.14$ W. Because the design value for $Q_{in} = 0.56$ W, measured Q_{in} is 1/4 of the design value. Two parameters appearing in Eq. 7 that were not measured or known accurately are k_m and k_{nm} the temperature-averaged thermal conductivities, respectively, of the Ag-Au substrate and brass. We therefore attribute this "pleasant" discrepancy (Q_{in} measured < Q_{in} design) to the uncertainties in the value of both k_m and k_{nm}.
- $2Q_{in}(I)$ is nearly independent of I — a slight increase, i.e., 0.4 W [= $2Q_{in}$ (6000 A) – $2Q_{in}(0)$], observed in the experiment is due chiefly to a fraction of a large dissipation taking place at the bottom HTS/Cu splice in each HTS section. As pointed out above, at 6000 A, the bottom HTS/Cu splice of each section is generating ~1.4 W or a total of ~2.8 W. Because each bottom splice is thermally well connected to its Nb_3Sn bus bar extension, it is reasonable to assume a fraction of it, ~0.2 W/section, enters into the LHe bath, thus making $2Q_{in}$ increase slightly with I.
- The temperatures of both the bottom and top ends of each HTS section are independent of I and remain, respectively, at ~4.2 K and ~77 K.
- As designed, unlike a *FullSuper* counterpart in which the HTS tapes operate in the fully superconducting state, $V(I)$ plots shown in Fig. 7 clearly show that the HTS tapes in each HTS section of this new pair of leads operate partially in the current-sharing mode. Because in an inevitable variation in $i_c(T_l)$ among 60 individual tape, each soldered with a brass strip, transition to the current-sharing region is not as defined as it would be if the values of $i_c(T_l)$ of 60 tapes were identical.

As may be inferred from Fig. 7, at 6000 A, resistive voltages due to the HTS tapes are 70 μV for the + section and 50 μV for the – section. In total these voltages generate 0.72 W. Since $2Q_{in}$(6000 A) – $2Q_{in}(0)$ is only 0.4 W even after attributing this to the generation at the two bottom HTS/Cu splices, we can confidently conclude that each HTS section successfully removes this "genuine" dissipation in the current-sharing region without increasing the heat input to the LHe as does the design calls for.

- LN2 flow rate required for operation agreed with that given by the design.

7. Conclusions

The experimental measurements have demonstrated that key performance data of the new 6-kA HTS-Copper leads agree reasonably well with those expected from design. We conclude that this new pair of 6-kA HTS-Copper leads to be a highly promising alternative for high-current leads that incorporate HTS.

Acknowledgement

This work was supported by the Post-doctoral Fellowship Program of Korea Science & Engineering Foundation (KOSEF)

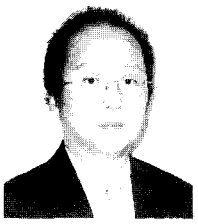

Haigun Lee
He was born in Chuncheon, Kangweon province, Korea. He received the B.S. degree in Materials Sci. & Eng. from Korea University, Seoul, Korea in 1987. He received the M.S. and the Ph.D degree in Materials Sci. & Eng. from University of Illinois, Chicago in 1990 and 1995, respectively. In 1990, he entered the Third Military Academy, Korea and he was appointed with the second lieutenant in 1991. From 1995-1997, he was a postdoctoral research associate at Francis Bitter Magnet Laboratory, Massachusetts Institute of Technology (MIT), where he is currently a research professor. Also he presently holds an appointment as a part-time researcher at American Magnetics, Inc, Oak Ridge, TN where he joined in 1999.

Ho Min Kim
He was born in Jeju-city, Jeju province, Korea. He received the B.S. degree in Electrical Engineering from Cheju National University, Jeju, Korea in 1995. He received the M.S. and the Ph.D degree in Electrical Engineering from Yonsei University, Seoul, Korea in 1998 and 2002, respectively. he is currently a postdoctoral research associate at Francis Bitter Magnet Laboratory, Massachusetts Institute of Technology (MIT).

References

[1] Yukikazu Iwasa and Haigun Lee, "High-temperature superconducting current lead incorporating operation in the current-sharing mode," *Cryogenics* 40, 209 (2000).
[2] Haigun Lee, Paul Arakawa, K. R. Efferson, R. Fielden, and Y. Iwasa, "AMI-MIT 1-KA leads with High-Temperature Superconducting Section – Design Concept and Key Parameters–", *IEEE Trans. on Applied Superconductivity*, Vol. 11, No. 1, March, p.2539 (2001).
[3] Yukikazu Iwasa Case Studies in Superconducting Magnets (Plenum Press, New York, 1994).
[4] A.F. Clark, G.E. Childs, and G.H. Wallace, "Electrical resistivity of some engineering alloys at low temperatures," *Cryogenics* 10, 295 (1970).

Yukikazu Iwasa
He was born in Kyoto, Japan. He received S.B and S.M. degrees in Mechanical Engineering and an S.M. degree in Electrical Engineering in 1962; an E.E. degree in Electrical Engineering in 1964; and a Ph.D. degree in Electrical Engineering in 1967, all from the Massachusetts Institute of Technology, Cambridge, MA. Except during a 1-year period 1966-1967 when he was a graduate student, he has been at the Francis Bitter Magnet Laboratory since 1964 specializing in superconducting magnet technology and cryogenic engineering. Currently he is Head of the Magnet Technology Division and research professor at FBML.

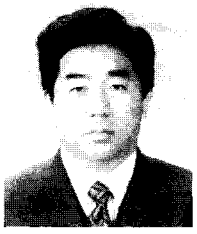

KeeMan Kim
He was born in Seoul, Korea, on November 18, 1960. He received the B.S. and the M.S. degree in nuclear engineering from Seoul national university, Seoul, Korea, in 1983 and 1985, and the Ph.D degree in nuclear engineering from University of Illinois at Urbana-Champaign, in 1989, respectively. During 1990-1994, he was a research at Argon National Laboratory (ANL), where he was involved in the R&D on large-scale magnet applications such as linear accelerator and tokamak. In 1994, he left ANL to join the Samsung Heavy Industries, where he had a responsibility for the development of the KSTAR CICC superconducing magnet. During 1996-2002, he moved to Samsung Electronics, where he had continuously worked for the development of the KSTAR magnet, and its test facility. He is currently working at Korea Basic Science Institute as a principal researcher for the development of KSTAR devices.

Paul Arakawa
He was born in Oak Ridge, Tennessee. He received the B.S. degree in mechanical engineering from Tennessee Technological University in 1983. From 1983-1991 he was a design engineer at Oak Ridge National Laboratory (ORNL). From 1991-1993, he was a program manager and design engineer at ORNL. In 1993, he took the role of Program Manager with the nuclear waste management division. In 1996, he left ORNL to join American Magnetics, Inc. where he is currently a senior magnet design engineer responsible for the design, fabrication, and testing of custom superconducting magnets and high current resistive and HTS current leads

Gregory J. Laughon
He was born in San Diego, California. He received a B.S. degree in Aerospace Engineering from San Diego State University in 1987. From 1988 to 1990, he worked as a test/cryogenic engineer at General Dynamics Space Systems Division. In 1990, he worked briefly for Rohr Industries as a mechanical design engineer working on aircraft engine nacelle designs. In 1991, he joined the Thermonuclear Fusion Research Group at General Atomics (GA) in San Diego as a principle cryogenic engineer. In 1997, he transitioned from the Fusion Group to the Accelerator Division at GA. In 2002, he moved to American Magnetics, Inc. to work as the Senior Cryogenic Engineer responsible for superconducting magnet cryostat design and custom current lead development.